J Therm Anal Calorim (2012) 108:1251–1260
DOI 10.1007/s10973-011-1945-3

Thermo-oxidative degradation kinetics and mechanism of the system epoxy nanocomposite reinforced with nano-Al_2O_3

Omid Zabihi · Abdollah Omrani · Abbas Ali Rostami

Received: 10 April 2011 / Accepted: 21 September 2011 / Published online: 7 October 2011

Abstract We have synthesized epoxy nanocomposites with various percents of nanoalumina by using ultrasonic dispersion treatment. Scanning calorimetry studies revealed that the composition having 1% nanoalumina results in the highest value of cross-link density as evidenced by the glass transition temperature (T_g). Thermal degradation of the systems consisting of diglycidyl ether bisphenol A (DGEBA)/1,3-Poropane diamine and with 1% and without nanoalumina were studied by thermogravimetry analysis to determine the reaction mechanism in air. The obtained results indicated that a relatively low concentration of nanoalumina led to an impressive improvement of thermal stability of epoxy resin. The Coats–Redfern, Van Krevelen, Horowitz–Metzger, and Criado methods were utilized to find the solid state thermal degradation mechanism. Analysis of our experimental results suggests that the reaction mechanism is depending on the applied thermal history. For the nanocomposite, the mechanism was recognized to be one-dimensional diffusion (D_1) reaction at low heating rates and it changes to be a random nucleation process with one nucleus on the individual particle (F_1) at high heating speeds. The results also indicated that the degradation mechanism of organic phase is influenced by the presence of inorganic nanofiller.

Keywords Thermal degradation kinetics · Kinetic models · Epoxy nanocomposite · TG

O. Zabihi · A. Omrani (✉) · A. A. Rostami
Faculty of Chemistry, University of Mazandaran,
P.O. Box 453, Babolsar, Mazandaran, Iran
e-mail: omrani@umz.ac.ir

Introduction

Epoxy resins were extensively used in the polymer industry for surface coatings, adhesives, painting materials, composites, laminates, and insulating materials for electric devices because they have good processing characters, chemical resistance, and low shrinkage on cure, superior electrical and mechanical properties, and good adhesion to many substrates. The reinforcement of polymers using fillers, whether inorganic or organic, is a common way to produce advanced materials. Conventional composites filled with nanometer size particles, fibers or platelets have been studied for many years to use in a large number of industrial applications. Epoxy resin reinforced with layered silicates has recently received increasing attention because of the possibility of obtaining improved properties in terms of stiffness, strength, fire resistance, dimensional stability, and shrinkage [1]. But unfortunately, the hydrophilic clay is not highly compatible with epoxy matrix. To improve their interfacial interaction, surface modification of the nanoclay by organic compounds is essential. The effect of intercalant on the polymerization of epoxy has been previously reported but only a few investigations were conducted on its influence on the mechanism and kinetics of cure [2, 3]. Knowledge concerning long-term behavior of high-performance composites is necessary for their applications in high temperature environments. Accordingly, degradation is even more crucial when the material is heated in an oxidizing atmosphere [4, 5]. Degradation of polymers includes some change in the chemical structure and physical properties because of external chemical or physical stresses. Bond scissions in the backbone of the macromolecules are an important resource of these types stress. The study of the degradation of an epoxy nanocomposite is important because it can determine the upper

temperature limit, the mechanism of a solid-state process, and the lifetime for the system. Thermal degradation kinetics of epoxy resin reinforced by various types of nanoscale fillers have been studied by means of thermogravimetric analysis [6–14].

The aim of this study is to obtain a global mechanism and mathematical model that accurately describes the decomposition kinetics of a pure epoxy and its nanocomposite. For this purpose, thermogravimetric curves were obtained at various heating rates for both the systems in air. The main objective is to answer this question: can the nanoalumina presence change the mechanism of thermal degradation? Since thermal and thermal-oxidative stabilities are related to the initial degradation temperature and the degradation rate of a polymer, determination of activation energy, and reaction order associated with degradation is an interesting topic. Therefore, we attempted here to explain the kinetics models which were used to evaluate the activation energy of the solid state thermal degradation.

Kinetic methods

Non-isothermal TG experiments record the change of the sample mass as a function of temperature. The kinetic parameters could be extracted from these experiments and the degree of conversion normally expresses as:

$$\alpha = \frac{m_0 - m}{m_0 - m_\infty} \tag{1}$$

where, m is the measured experimental mass at temperature T, m_0 is the initial mass, and m_∞ is the mass at the end of non-isothermal trace. The rate of conversion, $\mathrm{d}\alpha/\mathrm{d}t$, is a linear function of a temperature-dependent rate constant, k, and a temperature-independent function of conversion according to the following relation:

$$\frac{\mathrm{d}\alpha}{\mathrm{d}t} = kf(\alpha) \tag{2}$$

By substituting the Arrhenius equation into Eq. 2 once can be writing:

$$\frac{\mathrm{d}\alpha}{\mathrm{d}t} = Af(\alpha)e^{-\frac{E}{RT}} \tag{3}$$

If the temperature of the sample is changed by a controlled and constant heating rate, $\beta = \mathrm{d}T/\mathrm{d}t$, the variation in the degree of conversion could be analyzed as a function of temperature. This temperature will be dependent on the time of heating. Therefore, the reaction rate might be explained as:

$$\frac{\mathrm{d}\alpha}{\mathrm{d}T} = \frac{A}{\beta}\mathrm{e}^{-\frac{E}{RT}}f(\alpha) \tag{4}$$

Integration of Eq. 4 from an initial temperature corresponding to a null degree of conversion, i.e., T_0, to the peak temperature of the derivative thermogravimetry curve (DTG), i.e., T_p, where $\alpha = \alpha_\mathrm{p}$ gives [15]:

$$g(\alpha) = \int_0^{\alpha_\mathrm{p}} \frac{\mathrm{d}\alpha}{f(\alpha)} = \frac{A}{\beta}\int_0^{T_\mathrm{p}} \mathrm{e}^{-\frac{E}{RT}}\mathrm{d}T \tag{5}$$

where, $g(\alpha)$ is the integral function of conversion. In the case of polymers, this integral function is either a sigmoidal or a deceleration function. These functions were satisfactorily employed for estimating the solid state reaction mechanism from non-isothermal TG experiments [16–18].

Differential methods

Kissinger's method [19]

The method of Kissinger has been used in the literature to determine the activation energy of various solid state reactions by plotting the logarithm of the heating rate versus temperature inverse at the maximum reaction rate. The activation energy can be determined without a precise knowledge of the reaction mechanism using the following equation:

$$\ln\left(\frac{\beta}{T_\mathrm{max}^2}\right) = \left\{\ln\frac{AR}{E} + \ln[n(1-\alpha_\mathrm{max})^{n-1}]\right\} - \frac{E}{RT_\mathrm{max}} \tag{6}$$

where, β is the heating rate, T_max is the temperature corresponding to the inflection point of the thermodegradation curve which corresponds to the maximum reaction rate, A is the pre-exponential factor, α_max is the maximum conversion, and n is the reaction order. A plot of $\ln(\beta/T_\mathrm{max}^2)$ versus $1000/T_\mathrm{max}$ allows calculating the activation energy from the slope as well.

Integral methods

The integral methods involve an approximate integration of Eq. 5. The methods which were employed in the present study are: Flynn–Wall–Ozawa, Coats–Redfern, Horowitz–Metzger, and Van Krevelen methods.

Flynn–Wall–Ozawa method [20, 21]

Using the Doyle approximation [22], the integration of Eq. 5 results in the following equation:

$$\log\beta = \log\left[\frac{AE}{g(\alpha)R}\right] - 2.315 - \frac{0.4567E}{RT} \tag{7}$$

where, β, A, E, and T have the known meanings. This is one of the integral methods that can determine the activation energy without knowledge of the reaction order. It was used to determine E by illustrating and following

fitting of ln β versus 1000/T plot for various degrees of conversions.

Coats–Redfern method [23]

The Coats–Redfern method has been found to be the most versatile approach to calculate the kinetic parameters of thermal degradation processes. The integration of Eq. 4 by the Coats–Redfern method provides the following relation:

$$\ln\frac{g(\alpha)}{T^2} = \ln\frac{AR}{\beta E} - \frac{E}{RT} \tag{8}$$

By plotting $\ln[g(\alpha)/T^2]$ versus 1000/T at a constant heating rate and by using a selected degradation function, the apparent activation energy and pre-exponential factor could be obtained.

Van Krevelen [24] and Horowitz–Metzger [25] methods

Van Krevelen made the first serious theoretical treatment of thermogravimetry data. He has approximated the exponential integral to obtain an equation in the following final form:

$$\log g(\alpha) = \log B + \left(\frac{E}{RT_r} + 1\right)\log T \tag{9}$$

where,

$$B = \frac{A}{\beta}\left(\frac{E}{RT_r} + 1\right)^{-1}\left(\frac{0.368}{T_r}\right)^{\frac{E}{RT_r}} \tag{10}$$

and T_r is a reference temperature. The Horowith–Metzger method simplifies the exponential integral using an approximation similar to the Van Krevelen assumption. By defining a characteristic temperature of θ as $\theta = T - T_r$ and using the following approximation:

$$\frac{1}{T} = \frac{1}{T_r + \theta} \cong \frac{1}{T_r} - \frac{\theta}{T_r^2} \tag{11}$$

They have finally obtained:

$$\ln g(\alpha) = \frac{E\theta}{RT_r^2} \tag{12}$$

It should be noted that this equation is valid for $n = 1$. Both the methods suffer the problem of an arbitrary selection of the reference temperature. In order to obtain reproducible results for the present study, the reference temperature was considered as that corresponding to the temperature of maximum rate of degradation. We have also assumed that the selection of this arbitrary temperature does not affect the integral approximation of the kinetic model. One advantage of these methods is that the activation energy could be determined without precise knowledge of the thermodegradation kinetics.

Criado et al. [26] method for determination of reaction mechanism

The activation energy of a solid state reaction could be determined from several non-isothermal measurements. If the value of the activation energy is known, the kinetic model of the process could be found by Criado method. Criado and co-workers have defined the function

$$z(\alpha) = \left(\frac{d\alpha}{dt}\right)\frac{T}{\beta}\pi(x) \tag{13}$$

where $x = E/RT$; and $\pi(x)$ is an approximation of the temperature integral which cannot be expressed in a simple analytical form. In this study we used the fourth rational expression of Senum and Young [27], which gives errors lower than 10^{-5}% for $x = 20$: Combination of Eqs. 1 and 13 yields

$$z(\alpha) = f(\alpha)g(\alpha) \tag{14}$$

This last equation was used to obtain the master curves as a function of the reaction degree corresponding to the different models listed in Table 1. Plotting of the $z(\alpha)$ function calculated by experimental data and Eq. 13, and comparing the results with the master curves leads to easy and precise determination of the mechanism of a solid state process.

Experimental

Materials

The epoxy system used in this study was diglycidyl ether bisphenol A (D.E.R 332) from Sigma Aldrich with an epoxy equivalent weight of 175 g eq^{-1}. The 1,3-Poropane diamine, molecular weight of 74.13 g mol^{-1}, was utilized as curing agent. The diamine was donated from Merck. Alumina nanoparticles (Mw = 101.96 g mol^{-1} in gamma phase) having an average size of 50 nm and surface area of

Table 1 Data from dynamic DSC measurements on the pure epoxy and its nanocomposites having different values of nano-Al_2O_3 at heating rate of 10 °C min^{-1}

Nano-Al_2O_3/%	ΔH_T/J g^{-1}	Peak cure onset/°C	T_g/°C	Peak cure max/°C
0	465.7	54	89	79
1	440.7	57	109	83
2.5	412.2	61	106	85
5	395.5	66	102	87
10	380.1	71	98	90
15	366.3	77	93	92

35–43 m^2 g^{-1} were purchased from Aldrich. All the used solvents were in analytical grad.

Sample preparation and curing cycle selection

To prepare the composites a specific level of nanoalumina was added into epoxy matrix before adding the curing agent at stoichiometric ratio. In a series of experiments, the amount of nanoalumina was chosen to be 1, 2.5, 5, 10, and 15% of the total mass of the compositions. Noticeably, the amount of nanoalumina was selected respect to the total value of resin/diamine mixture. An ultrasonic mixing process (Viasonic Cavitation) was employed to disperse the nanoparticles into the resin matrix. Bulk samples of 1000 mg were prepared and kept in a refrigerator before the measurements. About 10 mg in size sample was used for DSC tests. For the TG experiments, epoxy resin and 1% nanoalumina were carefully and homogeneously mixed, and then the curing agent added at stoichiometric ratio. The mixtures were safely introduced into a cylindrical frame and finally the curing reaction conducted according to the following schedule: (step 1) Curing the compositions in an oven at 70 °C for 60 min, (step 2) Postcuring of the samples at 120 °C for 45 min. This curing cycle has been chosen according to the data obtained by scanning calorimetry measurements.

Measurements

Differential scanning calorimetry (DSC) measurements were performed using a DSC-60 (Shimadzu, Japan) calorimeter in high purity nitrogen atmosphere. The samples were heated in the temperature range of 25–300 °C at heating rate of 10 °C min^{-1} and then cooled to 25 °C to minimize the enthalpy relaxation. The calorimeter was calibrated using indium standard before the measurements. A re-scan treatment at low heating rate of 2 °C min^{-1} was used to estimate the glass transition temperature of the fully cured materials. From the observed exotherms, the total reaction enthalpy and the peak temperature were also determined.

TG tests were carried out using a Thermogravimetry Analyzer (TGA-50, Shimadzu, Japan). The microbalance was calibrated to prevent the discontinuous change in the magnetic properties on heating. The Curie point of Nickel and Perk-alloy was used to temperature calibration. Since most of the thermal degradation processes in nature occurs in static air, thermogravimetry experiments was conducted in air atmosphere. The system was operated in a dynamic mode and the temperature range of the experiments was between 25 and 750 °C at heating rates of 2.5, 5, 7.5, 10, and 15 °C min^{-1}. The sample mass was about 10 mg.

Results and discussion

Calorimetry studies

Data from scanning DSC measurements were listed in Table 1. From this thermal information the optimum level of nanoalumina was determined to be 1%.

Analysis of the DSC thermograms exhibits that the reaction heat of DGEBA/diamine system including 1% of the nanofiller is lower than that of the pure epoxy system and its value decreases by increasing nanoalumina concentration (See Table 1). One point which may clearly be implied from this observation is that high concentration of nanoalumina has a converse effect on heat evolution during the course of reaction. This may be because of the formation of aggregated zones in the resin matrix as the result of poor compatibility between the organic and inorganic phases in hybrid materials. The aggregated area will

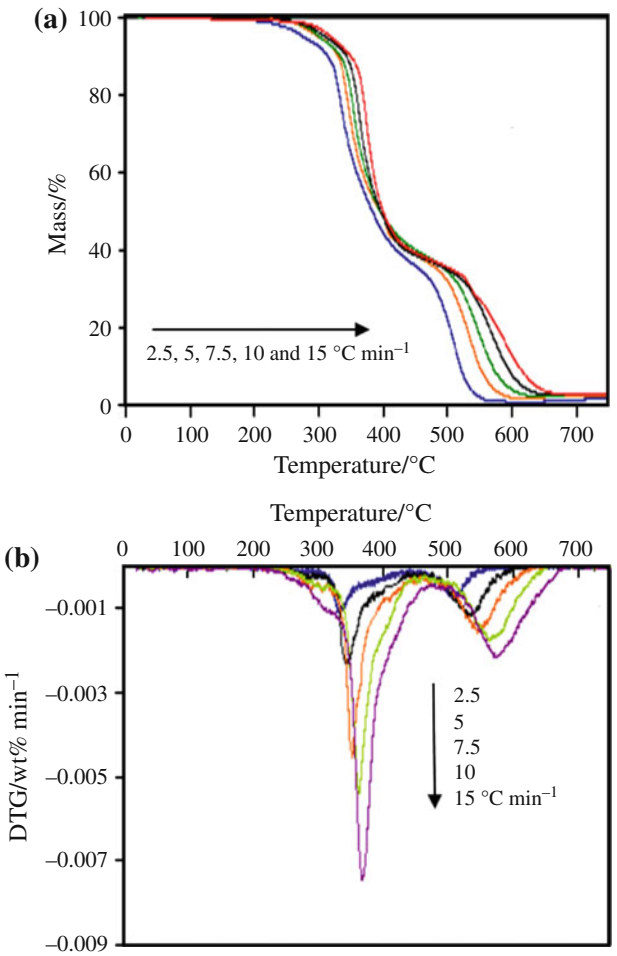

Fig. 1 TG (**a**) and DTG (**b**) curves of the epoxy nanocomposite recorded at various heating rates of 2.5, 5, 7.5, 10, and 15 °C min^{-1} in air

actually act as a barrier to heat evolution. More importantly, we have also observed that the reproducible results were those corresponding to the compositions having low level of nanoalumina loadings.

Also, the T_g of the nanocomposites is higher than that of the pure epoxy system and its value decreases at concentrations higher than 1 phr. The decrease in the T_g is because of interfacial interactions between alumina nanoparticles and polymer chains. Possible interfacial integrations are hydrogen bonding, van der Walls forces, and electrostatic forces.

Thermogravimetry studies

Characterization of TG thermograms and thermal stability assessment

The TG data of the pure epoxy and its nanocomposite were obtained at five different heating rates of 2.5, 5, 7.5, 10, and 15 °C min^{-1}. Figure 1a exhibits the curves of mass loss against temperature at various heating rates for the nanocomposite. The corresponding differential thermograms (DTG) were also shown in Fig. 1b.

Thermal degradation of the nanocomposite showed two degradation stages: The first degradation was occurred at about 350 °C and the second one observed at temperature higher than 500 °C. We have attempted to make a correlation between the observed losses in mass in both the steps and specific thermal events in the system. Accordingly, we have recorded TG curve of the sole nanoalumina in the same temperature range. As it is shown in Fig. 2, a single mass loss phenomenon at the same temperature range corresponds to the second stage of Fig. 1 was seen. Therefore, a thermal phenomenon in pure nanoalumina has a contribution to the second step thermal event observed in Fig. 1, clearly.

We think this phenomenon may be related to the calcination of the nanoparticle. To gain more insights about the observed thermal events, TG and DTG curves of the pure epoxy system, i.e., without nanofiller, at different heating rates were also recorded and the results presented in Fig. 3a and b.

More interestingly, the thermograms showed a two-step thermal degradation pattern. Again, the second step was appeared at approximately same temperature interval of those peaks observed in Figs. 2 and 1b. At least, these observations verify that the second stage in the TG curves of the epoxy nanocomposite is not because of a sole thermal event. Contributions from the nanoalumina calcination and thermal decomposition of the epoxy network should be existed, simultaneously. In general, these curves are D type [28], which corresponds to a two-stage decomposition reaction. A plot of conversion versus temperature and

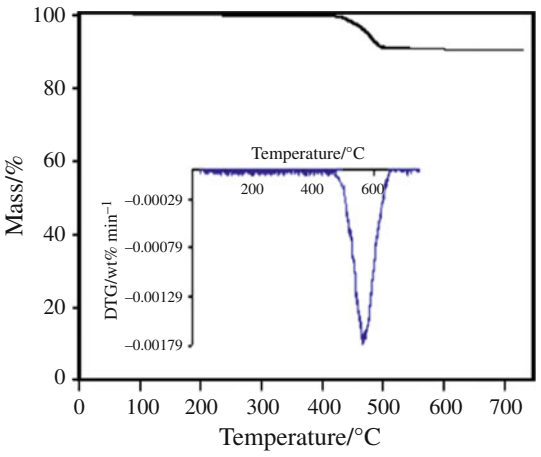

Fig. 2 TG and DTG curves of the alumina nanoparticles: temperature range 25–750 °C, in static air atmosphere, and at heating rate of 10 °C min^{-1}

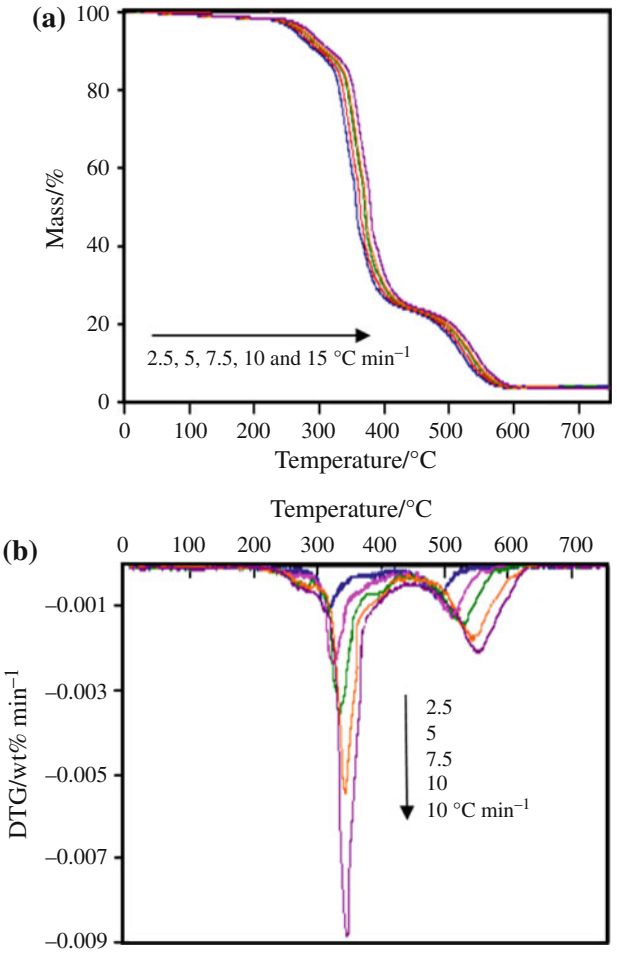

Fig. 3 TG (**a**) and DTG (**b**) curves of the pure epoxy recorded at various heating rates of 2.5, 5, 7.5,10, and 15 °C min^{-1} in air

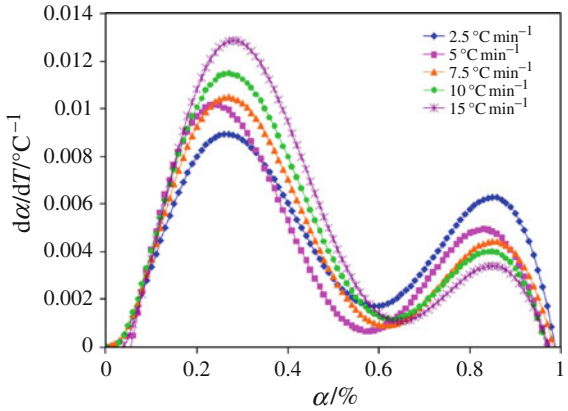

Fig. 4 Plot of $d\alpha/dT$ as a function of α and β for the dynamic degradation of the epoxy nanocomposite

heating rate for the nanocomposite was generated in Fig. 4. This figure shows that the contribution of the first stage in the total mass loss will increase by increasing heating rate. This means that a fast heating treatment results in promoted thermal degradation at the same temperature interval. To compare the thermal stability of the produced materials, we analyzed the TG curves by defining a few parameters, such as $T_{initial}$ and $W_{residual}$. The result of our analysis was collected in Table 2. In this Table, $T_{initial}$ and T_{final} show the temperatures at which the loss in mass of the materials is 5 and 95%, respectively. Thermal stability of the materials was also evaluated by determining chair yield at 750 °C as nominated by values of $W_{residual}$ in Table 2.

In addition, the $T_{initial}$ provides good idea about the beginning of the thermal degradation. By inspecting the data in Table 2 one can be concluded that the residual mass was decreased by increasing the heating rate for both the

Table 2 TG data of the thermal degradation at different heating rates

Heating rate/°C min^{-1}	$T_{initial}$/°C	T_{final}/°C	T_{max}/°C	$W_{residue}$/%
Nanocomposite				
2.5	279	519	332	8.32
5	299	549	342	8.05
7.5	305	569	353	7.76
10	311	591	364	7.16
15	320	601	368	6.89
Pure epoxy				
2.5	263	548	313	6.89
5	268	554	325	6.64
7.5	275	561	335	6.24
10	279	565	344	5.95
15	286	571	349	5.79

$T_{initial}$ is the temperature at 5% lose in mass, T_{final} is the temperature at 95% mass loss, T_{max} is the temperature at inflection point, and the $W_{residual}$ is the residual mass after complete degradation at 750 °C

systems. So, the nanofiller have a significant influence on the thermal stability of the epoxy nanocomposite and this effect will be increased by increasing the heating rate. The difference between the $T_{initial}$ values of the pure epoxy and its nanocomposite is 34 °C at 15 °C min^{-1} ,while this value is only 16 °C at low heating rate of 2.5 °C min^{-1}. In order to eliminate the influence of heating rates on thermal degradation, T_{max} was taken as an example to quantitative analysis. As shown in Fig. 5, T_{max} of pure epoxy and nanocomposite increased linearly along with the heating rates. The relationship between T_{max} and β could be expressed as the following equation:

$$T_{max} = A\beta + T^0_{max} \quad (15)$$

where, T^0_{max} is the equilibrium peak thermal degradation temperature by assuming that the heating rate equals 0 °C min^{-1}, and A is the rate constant [29]. The T^0_{max} of nanocomposite increased by 17.8 °C in contrast to that of the pure epoxy indicating that the presence of nanoalumina increases the thermal stability of the nanocomposite.

Theoretically, the higher A value is owing to the better barrier properties. The A value of the nanocomposite is higher which may be described by the fact that the nanocomposite has more improved thermal transport barrier effect than the pure epoxy.

Determination of activation energy and kinetic model

The Kissinger method was first utilized to analyze the TG data because it is independent of any pre-assumption about the thermal degradation mechanism. The activation energy for both the examined epoxy systems were calculated from straight line fitting of $\ln(\beta/T^2_{max})$ versus $1000/T_{max}$ plots (See Fig. 6). The values obtained for the activation energy were 175.4 and 125.8 kJ mol^{-1} for the nanocomposite and pure epoxy systems, respectively. Obviously, the presence of

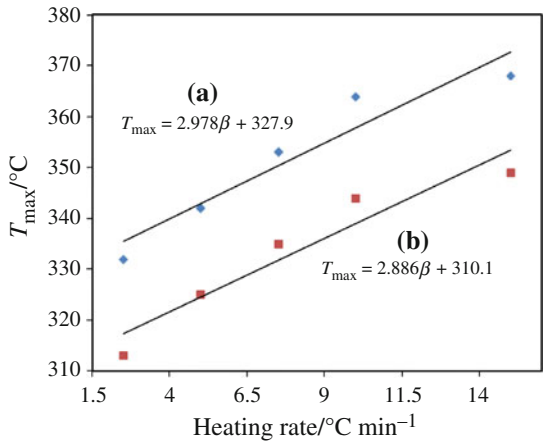

Fig. 5 The plot of T_{max} versus heating rates of epoxy nanocomposite (**a**) and pure epoxy (**b**)

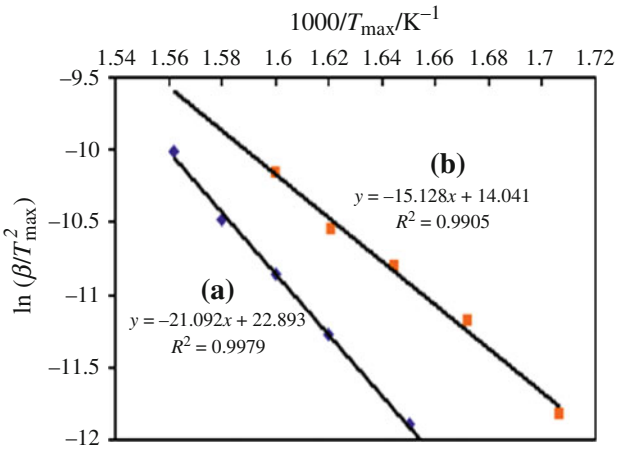

Fig. 6 The Kissinger plots for the nanocomposite (**a**) and pure epoxy (**b**) system

Table 3 Activation energies obtained using the Flynn–Wall–Ozawa Method (R^2 = 0.98–0.99)

α/%	E_a/kJ mol^{-1}	
	Nanocomposite	Pure epoxy
20	154.7	91.0
23	161.1	109.2
26	172.4	127.4
29	181.6	136.5
32	197.9	159.9
35	205.7	160.2
Average	178.9	129.5

the nanofiller increased the activation energy of the thermal decomposition process demonstrating lower decomposition rate.

The activation energy was also evaluated by the iso-conversional method of Flynn–Wall–Ozawa by generating linear plots of ln β versus 1000/T at various conversions. Owing to the fact that this equation was derived using the Doyle approximation, only conversions values in the range of 20–35% can be used. For the present study, the conversion values of 20, 23, 26, 29, 32, and 35% were examined. Results showed that the straight lines are nearly parallel indicating the applicability of the method to both the systems in the selected conversion range is reliable. This fact suggests that a single reaction mechanism should be operative in the systems [30–32]. Activation energies corresponding to the different conversions levels of both the systems were listed in Table 3. From these results, the mean values of 178.9 and 129.6 kJ mol^{-1} were found for the nanocomposite and pure epoxy systems, correspondingly.

Through analyzing the results obtained by the two methods, it was understood that the values were close to each other suggesting that the obtained values determine the range of activation energy, reasonably. However, the results corresponding to 26% conversion are very close to those values obtained by the Kissinger method.

Some authors [33–35] have used the activation energy obtained by these two approaches to find a suitable model describing thermo-degradation mechanism. In order to investigate the solid-state degradation mechanism in our study, the Coats–Redfern and Van Krevelen algorithms were selected as they both involved the mechanism in the

Table 4 Activation energies (kJ mol^{-1}) obtained using the Coats–Redfern method for several solid state processes at different heating rates for epoxy nanocomposite (a) and pure epoxy (b) (R^2 = 0.97–0.99)

Heating rate	2.5/°C min^{-1}		5/°C min^{-1}		7.5/°C min^{-1}		10/°C min^{-1}		15/°C min^{-1}	
Mechanism	(a)	(b)	(a)	(b)	(a)	(b)	(a)	(b)	(a)	(b)
A_2	45.4	160.4	46.2	163.9	62.2	170.5	82.7	179.4	79.7	186.5
A_3	27.3	122.2	28.1	125.4	38.5	127.2	51.8	129.9	49.6	136.3
A_4	18.2	230.5	18.9	245.8	26.6	253.5	36.3	264.6	34.6	281.4
R_1	83.7	285.3	84.4	299.6	112.1	308.5	147.2	321.3	143.0	335.5
R_2	91.6	302.8	92.1	320.6	122.4	336.8	160.9	348.4	156.3	367.2
R_3	94.3	311.2	94.9	347.5	125.9	363.9	165.6	376.8	160.8	398.6
D_1	176.2	485.8	176.8	503.6	233.0	510.7	304.6	524.3	296.9	545.4
D_2	186.5	504.7	187.1	527.6	245.4	543.8	322.3	556.7	313.6	573.2
D_3	197.5	517.4	198.0	545.5	260.9	562.6	341.6	574.8	332.7	597.5
F_1	99.9	397.5	100.3	403.7	133.0	409.7	175.0	414.5	169.7	432.7
F_2	25.5	224.9	26.1	245.4	35.8	267.6	49.2	285.9	46.2	301.4
F_3	59.9	368.6	60.6	389.8	80.5	406.5	108.5	412.4	103.3	435.7

solid state. According to Eq. 8 proposed by Coats–Redfern, the activation energy for each $g(\alpha)$ function could be calculated at a constant heating rate from fitting of $\ln[(g(\alpha))/T^2]$ versus $1000/T$ plots. Table 4 collects the activation energies in the conversion range of 20–35% at various heating rates for the pure epoxy system and its nanocomposite. Analysis of the data for the epoxy nanocomposite showed that at low heating rates of 2.5 and 5 °C min^{-1}, the activation energies were in better agreement with those values obtained using Kissinger's method, corresponds to a D_1 type mechanism. Noticeably, at other examined heating rates, the activation energies were in better concordance with those amounts determined using the method of Kissinger corresponds to an F_1 type mechanism. The same analytical treatment was used to characterize the mechanism of thermal degradation for the pure epoxy system. Accordingly, analysis of the data related to the pure epoxy system exhibits that the activation energies were in better conformity with those calculated by Kissinger's method, corresponds to an A_3 type mechanism at all the heating rates used.

To further support of the proposed degradation mechanisms, we have also calculated activation energies using the Van Krevelen and Horowith–Metzger models corresponding to mechanisms of D_n and F_n for the nanocomposite and A_n mechanism for the pure epoxy system. Using Eq. 9, the activation energy was obtained through a linear fitting of log $g(\alpha)$ versus log T plots. Table 5 shows activation energy at various heating rates for the nanocomposite. Obviously, D_1 mechanism at low heating rate (2.5 °C min^{-1}) and F_1 mechanism at high heating speed (15 °C min^{-1}) gives the numerical values which are in better agreement with those determined by Kissinger's method. Also, the results of our analysis on the pure epoxy system were listed in Table 5 revealing that the activation energies and correlations corresponding to A_3 mechanism were in good agreement to the value determined previously.

The values of activation energies and corresponding correlations obtained using the Horowitz–Metzger model for D_n and F_n mechanisms for the nanocomposite system were shown in Table 6. Again, the best agreement achieved to the Kissinger method corresponds to a D_1 mechanism at low (2.5 °C min^{-1}) and F_1 mechanism at high (15 °C min^{-1}) heating rates. When the data of pure epoxy system was analyzed by the Horowitz–Metzger equation (See Table 6), it was found that the best agreement to the Kissinger value is corresponds to an A_3 mechanism.

In order to confirm the conclusions, the master curve plots of $z(\alpha)$ versus α% for different mechanisms according to the Criado method have been illustrated in Fig. 7 for the systems under study at different heating rates. It clearly shows that the experimental data of $z(\alpha)$ of the pure epoxy at high and low heating rates agree with the A_3 master curve very well. At the same time, the experimental data of $z(\alpha)$ of epoxy nanocomposite at high and low heating rates agree with the F_1 and D_1 master curves, respectively.

Therefore, the thermo-oxidative degradation mechanism for the produced nanocomposite most probably followed a deceleration curves (D_n type) and its rate-controlling process obeyed the one-dimensional diffusion reaction at low heating rate. However, random nucleation (F_1 mechanism) having one nucleus on the individual particle will be the most convenient thermal degradation mechanism at high heating rates. The pure epoxy system showed different thermo-degradation mechanism most probably followed a sigmoidal curve (A_n type mechanism), a nucleation and growth mechanism having the rate-controlling step obeyed the Avrami-Erofeev equation.

Table 5 Activation energies (kJ mol^{-1}) obtained using the Van Krevelen method for various solid state processes for the pure epoxy and its nanocomposite ($R^2 = 0.97$–0.99)

Mechanism	2.5/°C min^{-1}	5/°C min^{-1}	7.5/°C min^{-1}	10/°C min^{-1}	15/°C min^{-1}
Epoxy nanocomposite					
D_1	209.4	223.3	251.7	351.6	284.9
D_2	221.4	236.1	266.1	371.6	300.9
D_3	234.2	249.8	281.6	393.3	318.2
F_1	121.0	129.1	145.9	204.7	165.9
F_2	35.2	37.7	43.3	62.4	48.4
F_3	75.4	80.5	91.8	130.1	102.0
Pure epoxy					
A_2	153.7	174.6	195.5	212.3	242.0
A_3	119.2	122.6	129.3	133.0	136.4
A_4	63.3	69.5	78.6	84.6	91.2

Table 6 Activation energies (kJ mol^{-1}) obtained using the Horowitz–Metzger method for various solid state processes for the pure epoxy and its nanocomposite ($R^2 = 0.97$–0.99)

Mechanism	2.5/°C min^{-1}	5/°C min^{-1}	7.5/°C min^{-1}	10/°C min^{-1}	15/°C min^{-1}
Epoxy nanocomposite					
D_1	198.7	221.7	262.3	323.9	298.6
D_2	209.7	233.9	276.9	342.1	315.0
D_3	221.8	247.5	293.2	362.0	333.1
F_1	116.8	130.2	154.4	160.6	175.
F_2	37.4	41.5	49.8	61.4	55.7
F_3	74.9	83.0	99.7	122.8	111.0
Pure epoxy					
A_2	283.5	301.7	326.1	386.0	398.3
A_3	126.3	134.6	145.2	160.8	171.4
A_4	45.3	58.6	67.3	78.9	90.3

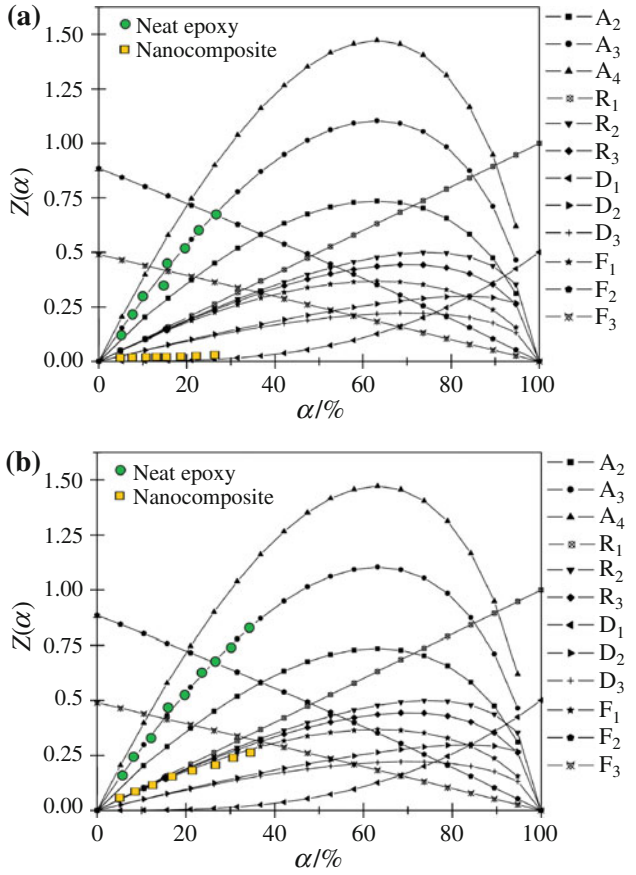

Fig. 7 Master plots for the pure epoxy and its nanocomposite at heating rate of **a** 2.5 °C min^{-1} and **b** 15 °C min^{-1}

Conclusions

A nanoalumina reinforced epoxy composite was produced and characterized by DSC technique. The nanocomposite was compared to the parent epoxy system in terms of its thermal stability and thermo-degradation kinetics and mechanism. Our results showed that these parameters of the studied solid state thermal degradation processes will be affected by the presence of the nanofiller. The corresponding kinetic parameters of the thermal degradation reactions were evaluated using the Kissinger and Flynn–Wall–Ozawa methods. The results also verified that the activation energy obtained by the two methods were in reliable agreement for the pure epoxy and nanocomposite systems. The Coats–Redrefn, Van Krevelen, Horowitz–Metzger, and Criado methods were utilized to discuss about the probable degradation mechanism of both the systems. The solid state decomposition mechanism of the nanocomposite was either F_1 or D_1 mechanism depending on the used heating rate. However, it was recognized that an A_3 type mechanism can describe the thermal decomposition mechanism of the system without nano-Al_2O_3, satisfactorily.

References

1. Brown JM, Curliss D, Vaia RA. Thermoset-layered silicate nanocomposites. Quaternary ammonium montmorillonite with primary diamine cured epoxies. Chem Mater. 2000;12(11):3376–84.
2. Roman F, Montserrat S, Hutchinson JM. On the effect of montmorillonite in the curing reaction of epoxy nanocomposites. J Therm Anal Calorim. 2007;87(1):113–8.
3. Pages P, Lacorte T, Lipinska M, Carrasco F. Study of curing of layered silicate/trifunctional epoxy nanocomposites by means of FTIR spectroscopy. J Appl Polym Sci. 2008;108(4):2107–15.
4. Tsotsis TK. Thermo-oxidative aging of composite materials. J Compos Mater. 1995;29(3):410–22.
5. Fan J, Hu X, Yue CY. Thermal degradation study of interpenetrating polymer network based on modified bismaleimide resin and cyanate ester. Polym Int. 2003;52:15–22.
6. Liu YL, Wei WL, Hsua KY, Ho WH. Thermal stability of epoxy-silica hybrid materials by thermogravimetric analysis. Thermochim Acta. 2004;412:139–47.
7. Aijuan G, Guozheng L. Thermal degradation behaviour and kinetic analysis of epoxy/montmorillonite nanocomposites. Polym Degrad Stab. 2003;80:383–91.
8. Sameer SR, Mauro Z, Szabolcs M, Krzysztof KK, Alan HW, Marc N, Takashi K, Jeffrey WG. Effect of carbon nanotubes and montmorillonite on the flammability of epoxy nanocomposites. Polym Degrad Stab. 2010;95:870–9.
9. Kuan CF, Chen WJ, Li YL, Chen CH, Kuan HC, Chiang CL. Flame retardance and thermal stability of carbon nanotube epoxy composite prepared from sol–gel method. J Phy Chem Solids. 2010;71:539–43.
10. Budrugeac P. Thermal degradation of glass reinforced epoxy resin and polychloroprene rubber: the correlation of kinetic parameters of isothermal accelerated aging with those obtained from non-isothermal data. Polym Degrad Stab. 2001;74:125–32.
11. Chatterjee A, Islam MS. Fabrication and characterization of TiO_2–epoxy nanocomposite. Mater Sci Eng A. 2008;487:574–85.
12. Sanctuary R, Baller J, Zielinski B, Becker N, Krüger JK, Philipp M, Müller U, Ziehmer M. Influence of Al_2O_3 nanoparticles on the isothermal cure of an epoxy resin. J Phys Condens Matter. 2009;21(3):035118.
13. Vassileva E, Friedrich K. Epoxy/alumina nanoparticle composites. II. Influence of silane coupling agent treatment on mechanical performance and wear resistance. J Appl Polym Sci. 2006;101:4410–7.
14. Baller B, Thomassey M, Ziehmer M, Sanctuary R. The catalytic influence of alumina nanoparticles on epoxy curing. Thermochim Acta. 2011;517(1–2):34–9.
15. Nunez L, Fraga F, Fraga L, Rodriguez JA. Activation energies and rate constants for an epoxy/cure agent reaction. Variation in peak exotherm temperature. J Therm Anal. 1996;47:743–50.
16. Ma S, Hill JO, Heng S. A kinetic analysis of the pyrolysis of some Australian coals by non-isothermal thermogravimetry. J Therm Anal. 1991;37:1161–77.
17. Sestak J, Berggren G. Study of the kinetics of the mechanism of solid-state reactions at increasing temperatures. Thermochim Acta. 1971;3:1–7.
18. Montserrat S, Malek J, Colomer P. Thermal degradation kinetics of epoxy–anhydride resins: I. Influence of a silica filler. Thermochim Acta. 1998;31:83–93.
19. Kissinger HE. Reaction kinetics in differential thermal analysis. Anal Chem. 1957;29:1702–6.
20. Flynn JH, Wall LA. A quick, direct method for the determination of activation energy from thermogravimetric data. J Polym Sci. 1966;4:323–42.

21. Ozawa T. A new method of analyzing thermogravimetric data. Bull Chem Soc Jpn. 1965;38(11):1881–6.
22. Doyle CD. Estimating thermal stability of experimental polymers by empirical thermogravimetric analysis. Anal Chem. 1961;33:77–9.
23. Coats AW, Redfern JP. Kinetic parameters from thermogravimetric data. Nature. 1964;201:68–75.
24. Van Krevelen DW, Van Heerden C, Huntjons FJ. Physicochemical aspects of the pyrolysis of coal and related organic compounds. Fuel. 1951;30:253–8.
25. Horowitz HH, Metzger G. A new analysis of thermogravimetric traces. Anal Chem. 1963;35(10):1464–8.
26. Criado JM, Malek J, Ortega A. Applicability of the master plots in kinetic analysis of non-isothermal data. Thermochim Acta. 1989;147:377–85.
27. Senum GI, Yang RT. Rational approximations of the integral of the Arrhenius function. J Therm Anal Calorim. 1977;11:445–7.
28. Hatakeyama T, Quinn FX. Thermal analysis: fundamentals and applications to polymer science. London: Wiley; 1999.
29. Zheng P, Li S, Huang M, Xu K, Wang C, Li P, Chen X. Thermogravimetric analysis of methyl methacrylate-graft-natural rubber. J Appl Polym Sci. 2002;85:2952–5.
30. Flynn JH. Degradation kinetics applied to lifetime predictions of polymers. Polym Eng Sci. 1980;20:675–7.
31. Flynn JH. Thermal analysis kinetics-problems, pitfalls and how to deal with them. J Therm Anal. 1988;34:367–81.
32. Ozawa T, Kato T. A simple method for estimating activation energy from derivative thermoanalytical curves and its application to thermal shrinkage of polycarbonye. J Therm Anal. 1991;37:1299–307.
33. Nunez L, Fraga F, Nunez MR, Castro A, Fraga L. Effects of diffusion on the kinetic study of the system BADGE $n = 0$/*m*-xylylenediamine. J Appl Polym Sci. 1999;74:2997–3005.
34. Jimenez A, Berenguer V, Lopez L, Sanchez A. Thermal degradation study of poly(vinyl chloride): kinetic analysis of thermogravimetric data. J Appl Polym Sci. 1993;50:1565–73.
35. Villanueva M, Martín-Iglesias JL, Rodríguez-Anón JA, Proupín-Castineiras J. Thermal study of an epoxy system DGEBA ($n = 0$)/MXDA with POSS. J Therm Anal. 2009;96:575–82.